CHAPTER 24
Finite Difference: Parabolic Equations

The previous chapter dealt with steady-state PDEs. We now turn to the parabolic equations that are employed to characterize time-variable problems. In the latter part of this chapter, we will illustrate how this is done in two spatial dimensions for the heated plate. Before doing this, we will first show how the simpler one-dimensional case is approached.

24.1 THE HEAT CONDUCTION EQUATION

In a similar fashion to the derivation of the Laplace equation (Eq. 23.6), conservation of heat can be used to develop a heat balance for the differential element in the long, thin insulated rod shown in Fig. 24.1. However, rather than examine the steady-state case, the present balance also considers the amount of heat stored in the element over a unit time period Δt. Thus, the balance is in the form, inputs − outputs = storage, or

$$q(x)\,\Delta y\,\Delta z\,\Delta t - q(x + \Delta x)\,\Delta y\,\Delta z\,\Delta t = \Delta x\,\Delta y\,\Delta z\,\rho C\Delta T$$

Dividing by the volume of the element ($=\Delta x\,\Delta y\,\Delta z$) and Δt gives

$$\frac{q(x) - q(x + \Delta x)}{\Delta x} = \rho C\,\frac{\Delta T}{\Delta t}$$

Taking the limit yields

$$-\frac{\partial q}{\partial x} = \rho C\,\frac{\partial T}{\partial t}$$

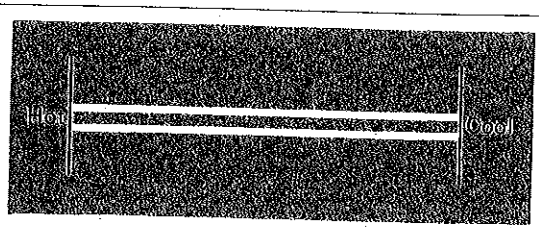

Figure 24.1
A thin rod, insulated at all points except at its ends.

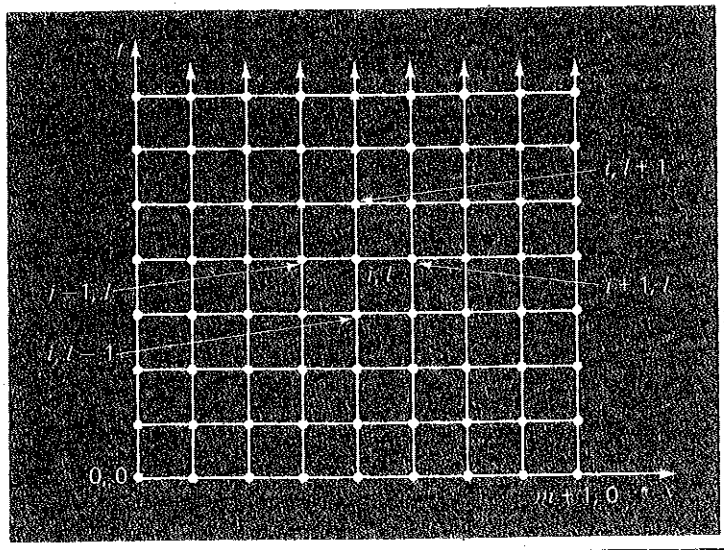

Figure 24.2
A grid used for the finite-difference solution of parabolic PDEs in two independent variables such as the heat-conduction equation. Note how, in contrast to Fig. 23.3, this grid is open-ended in the temporal dimension.

Substituting Fourier's law of heat conduction [Eq. (23.4)] results in

$$k \frac{\partial^2 T}{\partial x^2} = \frac{\partial T}{\partial t} \tag{24.1}$$

which is the *heat-conduction equation*.

Just as with elliptic PDEs, parabolic equations can be solved by substituting finite divided differences for the partial derivatives. However, in contrast to elliptic PDEs, we must now consider changes in time as well as in space. Whereas elliptic equations were bounded in all relevant dimensions, parabolic PDEs are temporally open-ended (Fig. 24.2). Because of their time-variable nature, solutions to these equations involve a number of new issues, notably stability. This, as well as other aspects of parabolic PDEs, will be examined in the following sections as we present two fundamental solution approaches—explicit and implicit schemes.

24.2 EXPLICIT METHODS

The heat-conduction equation requires approximations for the second derivative in space and the first derivative in time. The former is represented in the same fashion as for the Laplace equation by a centered finite divided difference:

$$\frac{\partial^2 T}{\partial x^2} = \frac{T_{i+1}^l - 2T_i^l + T_{i-1}^l}{\Delta x^2} \tag{24.2}$$

which has an error (recall Fig. 17.3) of $O[(\Delta x)^2]$. Notice the slight change in notation that superscripts are used to denote time. This is done so that a second subscript can be used to designate a second spatial dimension when the approach is expanded to the two-dimensional case.

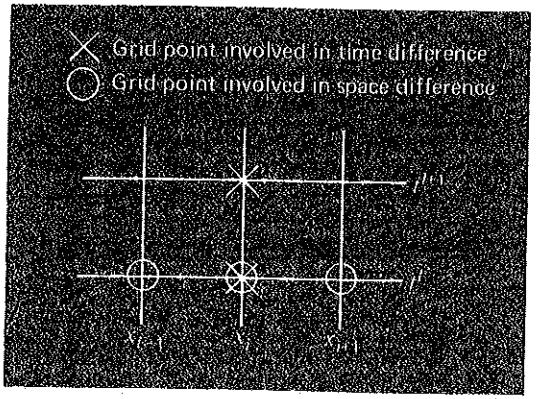

Figure 24.3
A computational molecule for the explicit form.

A forward finite divided difference is used to approximate the time derivative

$$\frac{\partial T}{\partial t} = \frac{T_i^{l+1} - T_i^l}{\Delta t} \tag{24.3}$$

which has an error (recall Fig. 17.1) of $O(\Delta t)$.

Substituting Eqs. (24.2) and (24.3) into Eq. (24.1) yields

$$k \frac{T_{i+1}^l - 2T_i^l + T_{i-1}^l}{(\Delta x)^2} = \frac{T_i^{l+1} - T_i^l}{\Delta t} \tag{24.4}$$

which can be solved for

$$T_i^{l+1} = T_i^l + \lambda(T_{i+1}^l - 2T_i^l + T_{i-1}^l) \tag{24.5}$$

where $\lambda = k\,\Delta t/(\Delta x)^2$.

This equation can be written for all the interior nodes on the rod. It then provides an explicit means to compute values at each node for a future time based on the present values at the node and its neighbors. In this sense, it is very similar to Euler's method for solving systems of ODEs. That is, if we know the temperature distribution as a function of position at $t = 0$, we can compute the distribution at Δt based on Eq. (24.5).

A computational molecule for the explicit method is depicted in Fig. 24.3, showing the nodes that constitute the spatial and temporal approximations. This molecule can be contrasted with others in this chapter to illustrate the differences between approaches.

EXAMPLE 24.1 Explicit Solution of the One-Dimensional Heat-Conduction Equation

Problem Statement: Use the explicit method to solve for the temperature distribution of a long, thin rod with a length of 10 cm and the following values: $k' = 0.49$ cal/(s·cm·°C), $\Delta x = 2$ cm, and $\Delta t = 0.1$ s. At $t = 0$, the temperature of the rod is zero and the boundary conditions are fixed for all times at $T(0) = 100$°C and $T(10) = 50$°C. Note that the rod is aluminum with $C = 0.2174$ cal/(g·°C) and $\rho = 2.7$ g/cm^3. Therefore, $k = 0.49/(2.7 \cdot 0.2174) = 0.835$ cm^2/s and $\lambda = 0.835(0.1)/(2)^2 = 0.020875$.

Solution: Applying Eq. (24.5) gives the following value at $t = 0.1$ s for the node at $x = 2$ cm:

$$T_1^1 = 0 + 0.020875\,[0 - 2(0) + 100] = 2.0875$$

At the other interior points, $x = 4$, 6, and 8 cm, the results are

$$T_2^1 = 0 + 0.020875\,[0 - 2(0) + 0] = 0$$

$$T_3^1 = 0 + 0.020875\,[0 - 2(0) + 0] = 0$$

$$T_4^1 = 0 + 0.020875\,[50 - 2(0) + 0] = 1.0438$$

At $t = 0.2$ s, the values at the four interior nodes are computed as

$$T_1^2 = 2.0875 + 0.020875\,[0 - 2(2.0875) + 100] = 4.0878$$

$$T_2^2 = 0 + 0.020875\,[0 - 2(0) + 2.0875] = 0.043577$$

$$T_3^2 = 0 + 0.020875\,[1.0438 - 2(0) + 0] = 0.021788$$

$$T_4^2 = 1.0438 + 0.020875\,[50 - 2(1.0438) + 0] = 2.0439$$

The computation is continued, and the results at 3-s intervals are depicted in Fig. 24.4. The general rise in temperature with time indicates that the computation captures the diffusion of heat from the boundaries into the bar.

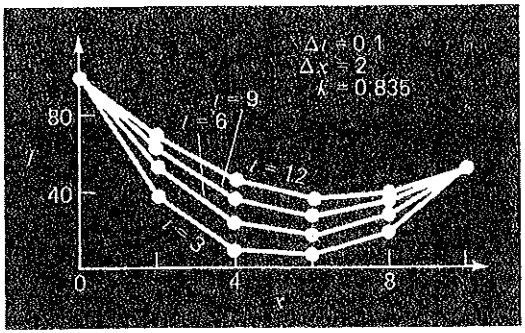

Figure 24.4
Temperature distribution in a long, thin rod as computed with the explicit method described in Sec. 24.2

24.2.1 Convergence and Stability

Convergence means that as Δx and Δt approach zero, the results of the finite-difference technique approach the true solution. *Stability* means that errors at any stage of the computation are not amplified but are attenuated as the computation progresses. It can

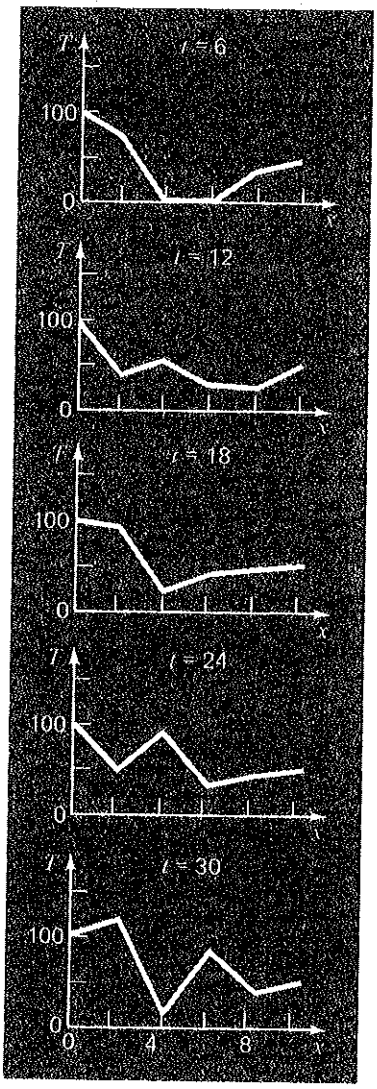

Figure 24.5
An illustration of instability. Solution of Example 24.1 but with $\lambda = 0.735$.

be shown (Carnahan et al., 1969) that the explicit method is both convergent and stable if $\lambda \leq 1/2$. Another way to formulate this criterion is

$$\Delta t \leq \frac{1}{2}\frac{\Delta x^2}{k} \tag{24.6}$$

In addition, it should be noted that setting $\lambda \leq 1/2$ could result in a solution in which errors do not grow but oscillate. Setting $\lambda \leq 1/4$ ensures that the solution will not oscillate. It is also known that setting $\lambda = 1/6$ tends to minimize truncation error (Carnahan et al., 1969).

Figure 24.5 is an example of instability caused by violating Eq. (24.6). This plot is for the same case as in Example 24.1 but with $\lambda = 0.735$ which is considerably greater than 0.5. As in Fig. 24.5, the solution undergoes progressively increasing oscillations. This situation will continue to deteriorate as the computation continues.

Although satisfaction of Eq. (24.6) will alleviate the instabilities of the sort manifested in Fig. 24.5, it also places a strong limitation on the explicit method. For example, suppose that Δx is halved to improve the approximation of the spatial second derivative. According to Eq. (24.6), the time step must be quartered to maintain convergence and stability. Thus, to perform comparable computations, the time steps must be increased by a factor of 4. Furthermore, the computation for each of these time steps will take twice as long because halving Δx doubles the total number of nodes for which equations must be written. Consequently, for the one-dimensional case, halving Δx results in an eightfold increase in the number of calculations. Thus, the computational burden may be large to attain acceptable accuracy. As will be described shortly, other techniques are available that do not suffer from such severe limitations.

24.2.2 Derivative Boundary Conditions

As was the case for elliptic PDEs (recall Sec. 23.3.1), derivative boundary conditions can be readily incorporated into parabolic equations. For a one-dimensional rod, this necessitates adding two equations to characterize the heat balance at the end nodes. For example, the node at the left end ($i = 0$) would be represented by

$$T_0^{l+1} = T_0^l + \lambda(T_1^l - 2T_0^l + T_{-1}^l)$$

Thus, an imaginary point is introduced at $i = -1$ (recall Fig. 23.8). However, as with the elliptic case, this point provides a vehicle for incorporating the derivative boundary condition into the analysis. Problem 24.1 at the end of the chapter deals with this exercise.

24.3 A SIMPLE IMPLICIT METHOD

As noted previously, explicit finite-difference formulations have problems related to stability. In addition, as depicted in Fig. 24.6, they exclude information that has a bearing on the solution. Implicit methods overcome both these difficulties at the expense of somewhat more complicated algorithms.

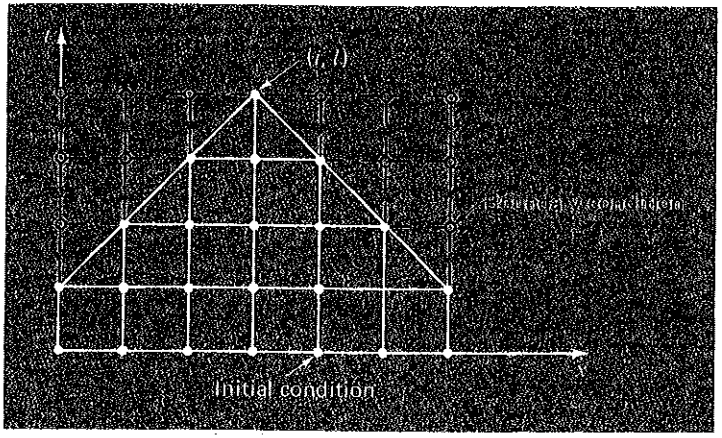

Figure 24.6
Representation of the effect of other nodes on the finite-difference approximation at node (i, l) using an explicit finite-difference scheme. The shaded nodes have an influence on (i, l) whereas the unshaded nodes, which in reality affect (i, l), are excluded.

The fundamental difference between explicit and implicit approximations is depicted in Fig. 24.7. For the explicit form, we approximate the spatial derivative at time level l (Fig. 24.7*a*). Recall that when we substituted this approximation into the partial differential equation, we obtained a difference equation (24.4) with a single unknown T_i^{l+1}. Thus, we can solve "explicitly" for this unknown as in Eq. (24.5).

In implicit methods, the spatial derivative is approximated at an advanced time level $l + 1$. For example, the second derivative would be approximated by (Fig. 24.7*b*)

$$\frac{\partial^2 T}{\partial x^2} \simeq \frac{T_{i+1}^{l+1} - 2T_i^{l+1} + T_{i-1}^{l+1}}{(\Delta x)^2} \tag{24.7}$$

which is second-order accurate. When this relationship is substituted into the original PDE, the resulting difference equation contains several unknowns. Thus, it cannot be solved explicitly by simple algebraic rearrangement as was done in going from Eq. (24.4) to (24.5). Instead, the entire system of equations must be solved simultaneously. This is possible because, along with the boundary conditions, the implicit formulations result in a set of linear algebraic equations with the same number of unknowns. Thus, the method reduces to the solution of a set of simultaneous equations at each point in time.

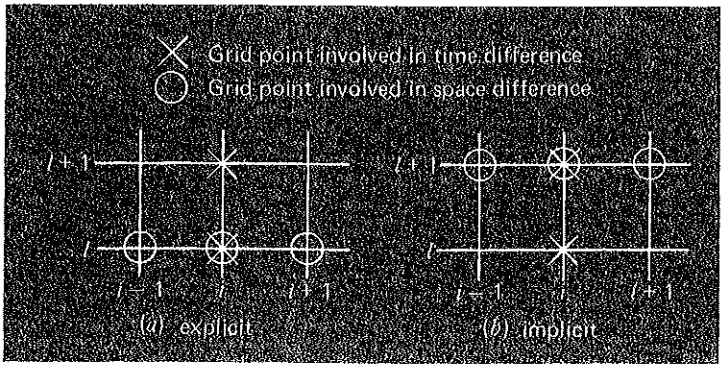

Figure 24.7
Computational molecules demonstrating the fundamental differences between (*a*) explicit and (*b*) implicit methods.

To illustrate how this is done, substitute Eqs. (24.3) and (24.7) into Eq. (24.1) to give

$$k\frac{T_{i+1}^{l+1} - 2T_i^{l+1} + T_{i-1}^{l+1}}{(\Delta x)^2} = \frac{T_i^{l+1} - T_i^l}{\Delta t}$$

which can be expressed as

$$-\lambda T_{i-1}^{l+1} + (1 + 2\lambda)T_i^{l+1} - \lambda T_{i+1}^{l+1} = T_i^l \tag{24.8}$$

where $\lambda = k\,\Delta t/(\Delta x)^2$. This equation applies to all but the first and the last interior nodes which must be modified to reflect the boundary conditions. For the case where the temperature levels at the ends of the rod are given, the boundary condition at the left end of the rod ($i = 0$) can be expressed as

$$T_0^{l+1} = f_0(t^{l+1}) \tag{24.9}$$

where $f_0(t^{l+1})$ is a function describing how the boundary temperature changes with time. Substituting Eq. (24.9) into Eq. (24.8) gives the difference equation for the first interior node ($i = 1$):

$$(1 + 2\lambda)T_1^{l+1} - \lambda T_2^{l+1} = T_1^l + \lambda f_0(t^{l+1}) \tag{24.10}$$

Similarly, for the last interior node ($i = m$),

$$-\lambda T_{m-1}^{l+1} + (1 + 2\lambda)T_m^{l+1} = T_m^l + \lambda f_{m+1}(t^{l+1}) \tag{24.11}$$

where $f_{m+1}(t^{l+1})$ describes the specified temperature changes at the right end of the rod ($i = m + 1$).

When Eqs. (24.8), (24.10), and (24.11) are written for all the interior nodes, the resulting set of m linear algebraic equations has m unknowns. In addition, the method has the added bonus that the system is tridiagonal. Thus, we can utilize the extremely efficient solution algorithms (recall Sec. 9.6) that are available for tridiagonal systems.

EXAMPLE 24.2 Simple Implicit Solution of the One-Dimensional Heat-Conduction Equation

Problem Statement: Use the simple implicit finite-difference approximation to solve the same problem as Example 24.1.

Solution: For the rod from Example 24.1, $\lambda = 0.020875$. Therefore, at $t = 0$, Eq. (24.10) can be written for the first interior node as

$$1.04175\,T_1^1 - 0.020875\,T_2^1 = 0 + 0.020875(100)$$

or

$$1.04175\,T_1^1 - 0.020875T_2^1 = 2.0875$$

In a similar fashion, Eqs. (24.8) and (24.11) can be applied to the other interior nodes. This leads to the following set of simultaneous equations:

$$\begin{bmatrix} 1.04175 & -0.020875 & & \\ -0.020875 & 1.04175 & -0.020875 & \\ & -0.020875 & 1.04175 & -0.020875 \\ & & -0.020875 & 1.04175 \end{bmatrix} \begin{Bmatrix} T_1^1 \\ T_2^1 \\ T_3^1 \\ T_4^1 \end{Bmatrix} = \begin{Bmatrix} 2.0875 \\ 0 \\ 0 \\ 1.04375 \end{Bmatrix}$$

which can be solved for the temperature at $t = 0.1$ s:

$$T_1^1 = 2.0047$$

$$T_2^1 = 0.0406$$

$$T_3^1 = 0.0209$$

$$T_4^1 = 1.0023$$

Notice how, in contrast to Example 24.1, all the points have changed from the initial condition during the first time step.

In order to solve for the temperatures at $t = 0.2$, the right-hand-side vector must be modified to account for the results of the first step as in

$$\begin{Bmatrix} 4.09215 \\ 0.04059 \\ 0.02090 \\ 2.04609 \end{Bmatrix}$$

The simultaneous equations can then be solved for the temperatures at $t = 0.2$ s:

$$T_1^2 = 3.9305$$

$$T_2^2 = 0.1190$$

$$T_3^2 = 0.0618$$

$$T_4^2 = 1.9653$$

Although the implicit method described is stable and convergent, it has the defect that the temporal difference approximation is first-order accurate whereas the spatial difference approximation is second-order accurate (Fig. 24.8). In the next section we present an alternative implicit method that remedies the situation.

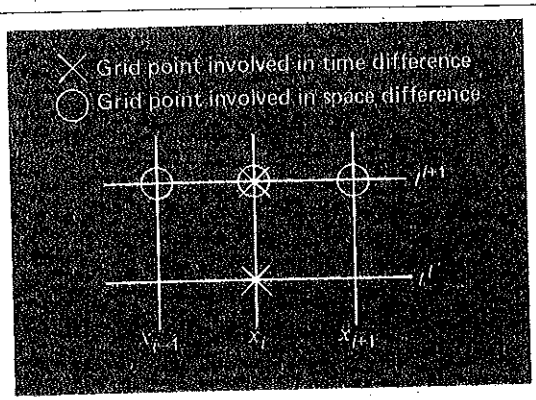

igure 24.8
computational molecule for
he simple implicit method.

24.4 THE CRANK-NICOLSON METHOD

The *Crank-Nicolson method* provides an alternative implicit scheme that is second-order accurate in both space and time. To provide this accuracy, difference approximations are developed at the midpoint of the time increment (Fig. 24.9). To do this, the temporal first derivative can be approximated at $t^{l+1/2}$ by

$$\frac{\partial T}{\partial t} \simeq \frac{T_i^{l+1} - T_i^l}{\Delta t} \tag{24.12}$$

The second derivative in space can be determined at the midpoint by averaging the difference approximations at the beginning (t^l) and at the end (t^{l+1}) of the time increment

$$\frac{\partial^2 T}{\partial x^2} \simeq \frac{1}{2}\left[\frac{T_{i+1}^l - 2T_i^l + T_{i-1}^l}{(\Delta x)^2} + \frac{T_{i+1}^{l+1} - 2T_i^{l+1} + T_{i-1}^{l+1}}{(\Delta x)^2}\right] \tag{24.13}$$

Substituting Eqs. (24.12) and (24.13) into Eq. (24.1) and collecting terms gives

$$-\lambda T_{i-1}^{l+1} + 2(1 + \lambda)T_i^{l+1} - \lambda T_{i+1}^{l+1} = \lambda T_{i-1}^l + 2(1 - \lambda)T_i^l + \lambda T_{i+1}^l \tag{24.14}$$

where $\lambda = k\,\Delta t/(\Delta x)^2$. As was the case with the simple implicit approach, boundary conditions of $T_0^{l+1} = f_0(t^{l+1})$ and $T_{m+1}^{l+1} = f_{m+1}(t^{l+1})$ can be prescribed to derive versions of Eq. (24.14) for the first and the last interior nodes. For the first interior node

$$2(1 + \lambda)T_1^{l+1} - \lambda T_2^{l+1} = \lambda f_0(t^l) + 2(1 - \lambda)T_1^l + \lambda T_2^l + \lambda f_0(t^{l+1}) \tag{24.15}$$

and for the last interior node

$$-\lambda T_{m-1}^{l+1} + 2(1 + \lambda)T_m^{l+1} = \lambda f_{m+1}(t^l) + 2(1 - \lambda)T_m^l + \lambda T_{m+1}^l + \lambda f_{m+1}(t^{l+1}) \tag{24.16}$$

Although Eqs. (24.14) through (24.16) are slightly more complicated than Eqs. (24.8), (24.10), and (24.11), they are also tridiagonal and, therefore, efficient to solve.

Figure 24.9
A computational molecule for the Crank-Nicolson method.

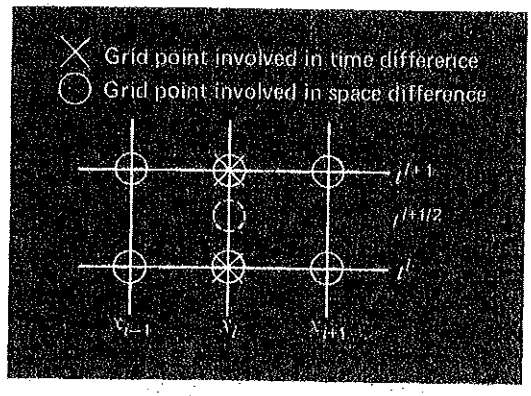

EXAMPLE 24.3 Crank-Nicolson Solution to the One-Dimensional Heat-Conduction Equation

Problem Statement: Use the Crank-Nicolson method to solve the same problem as in Examples 24.1 and 24.2.

Solution: Equations (24.14) through (24.16) can be employed to generate the following tridiagonal set of equations:

$$\begin{bmatrix} 2.01475 & -0.020875 & & \\ -0.020875 & 2.01475 & -0.020875 & \\ & -0.020875 & 2.01475 & -0.020875 \\ & & -0.020875 & 2.01475 \end{bmatrix} \begin{Bmatrix} T_1^1 \\ T_2^1 \\ T_3^1 \\ T_4^1 \end{Bmatrix} = \begin{Bmatrix} 4.175 \\ 0 \\ 0 \\ 2.0875 \end{Bmatrix}$$

which can be solved for the temperatures at $t = 0.1$ s:

$$T_1^1 = 2.0450$$

$$T_2^1 = 0.0210$$

$$T_3^1 = 0.0107$$

$$T_4^1 = 1.0225$$

In order to solve for the temperatures at $t = 0.2$ s, the right-hand-side vector must be changed to

$$\begin{Bmatrix} 8.1801 \\ 0.0841 \\ 0.0427 \\ 4.0901 \end{Bmatrix}$$

The simultaneous equations can then be solved for

$$T_1^2 = 4.0073$$

$$T_2^2 = 0.0826$$

$$T_3^2 = 0.0422$$

$$T_4^2 = 2.0036$$

24.4.1 Comparison of One-Dimensional Methods

Equation (24.1) can be solved analytically. For example, a solution is available for the case where the rod's temperature is initially at zero. At $t = 0$, the boundary condition at $x = L$ is instantaneously increased to a constant level of $\bar{T}$ while $T(0)$ is held at zero. For this case, the temperature can be computed by (Jenson and Jeffreys, 1977)

$$T = \bar{T}\left[\frac{x}{L} + \sum_{n=0}^{\infty} \frac{2}{n\pi}(-1)^n \sin\left(\frac{nx}{L}\right) \exp\left(\frac{-n^2\pi^2 kt}{L^2}\right)\right] \tag{24.17}$$

where L is the total length of the rod. This equation can be employed to compute the evolution of the temperature distribution for each boundary condition. Then, the total solution can be determined by superposition.

EXAMPLE 24.4 Comparison of Analytical and Numerical Solutions

Problem Statement: Compare the analytical solution from Eq. (24.17) with numerical results obtained with the explicit, simple implicit, and Crank-Nicolson techniques. Perform the comparison for the rod employed in Examples 24.1, 24.2, and 24.3.

Solution: Recall from the previous examples that $k = 0.835$ cm^2/s, $L = 10$ cm, and $\Delta x = 2$ cm. For this case, Eq. (24.17) can be used to predict that the temperature at $x = 2$ cm and $t = 10$ s would equal 64.8018. Table 24.1 presents numerical predictions of $T(2, 10)$. Notice that a range of time steps are employed. These results indicate a number of properties of the numerical methods. First, it can be seen that the explicit method is unstable for high values of λ. This instability is not manifested by either implicit approach. Second, the Crank-Nicolson method converges more rapidly as λ is decreased and provides moderately accurate results even when λ is relatively high. These outcomes are as expected because Crank-Nicolson is second-order accurate with respect to both independent variables. Finally, notice that as λ decreases, the methods seem to be converging on a value of 64.73 that is different than the analytical result of 64.80. This should not be surprising because a fixed value of $\Delta x = 2$ is used to characterize the x dimension. If both Δx and Δt were decreased as λ was decreased (that is, more spatial segments were used), the numerical solution would more closely approach the analytical result.

TABLE 24.1 **Comparison of three methods of solving a parabolic PDE: the heated rod. The results shown are for temperature at $t = 10$ s at $x = 2$ cm, for the rod from Example 24.1 through 24.3. Note that the analytical solution is $T(2,10) = 64.8018$.**

Δt	λ	Explicit	Implicit	Crank-Nicolson
10	2.0875	208.75	53.01	79.77
5	1.04375	−9.13	58.49	64.79
2	0.4175	67.12	62.22	64.87
1	0.20875	65.91	63.49	64.77
0.5	0.104375	65.33	64.12	64.74
0.2	0.04175	64.97	64.49	64.73

As indicated by the previous example, the Crank-Nicolson method is the preferred numerical method for solving parabolic PDEs in one spatial dimension. Its advantages become even more pronounced for more complicated applications such as those involving

unequally spaced meshes. Such nonuniform spacing is often advantageous where we have foreknowledge that the solution varies rapidly in local portions of the system. Further discussion of such applications and the Crank-Nicolson method in general can be found elsewhere (Ferziger, 1981; Lapidus and Pinder, 1982).

24.5 PARABOLIC EQUATIONS IN TWO SPATIAL DIMENSIONS

The heat-conduction equation can be applied to more than one spatial dimension. For two dimensions, its form is

$$\frac{\partial T}{\partial t} = k\left(\frac{\partial^2 T}{\partial x^2} + \frac{\partial^2 T}{\partial y^2}\right) \tag{24.18}$$

One application of this equation is to model the temperature distribution on the face of a heated plate. However, rather than characterizing its steady-state distribution, as was done in Chap. 23, Eq. (24.18) provides a means to compute the plate's temperature distribution as it changes in time.

24.5.1 Standard Explicit and Implicit Schemes

An explicit solution can be obtained by substituting finite-difference approximations of the form of Eqs. (24.2) and (24.3) into Eq. (24.18). However, as with the one-dimensional case, this approach is limited by a stringent stability criterion. For the two-dimensional case, the criterion is (Davis, 1984)

$$\Delta t \leq \frac{1}{8}\frac{(\Delta x)^2 + (\Delta y)^2}{k}$$

Thus, for a uniform grid ($\Delta x = \Delta y$), $\lambda = k\,\Delta t/(\Delta x)^2$ must be less than or equal to 1/4. Consequently, halving the step size results in a fourfold increase in the number of nodes and a 16-fold increase in computational effort.

As was the case with one-dimensional systems, implicit techniques offer alternatives that guarantee stability. However, the direct application of implicit methods such as the Crank-Nicolson technique leads to the solution of $m \times n$ simultaneous equations. Additionally, when written for two or three spatial dimensions, these equations lose the valuable property of being tridiagonal. Thus, matrix storage and computation time can become exorbitantly large. The method described in the next section offers one way around this dilemma.

24.5.2 The A.D.I. Scheme

The *alternating-direction implicit* or *A.D.I. scheme* provides a means for solving parabolic equations in two spatial dimensions using tridiagonal matrices. To do this, each time increment is executed in two steps (Fig. 24.10). For the first step, Eq. (24.18) is approximated by

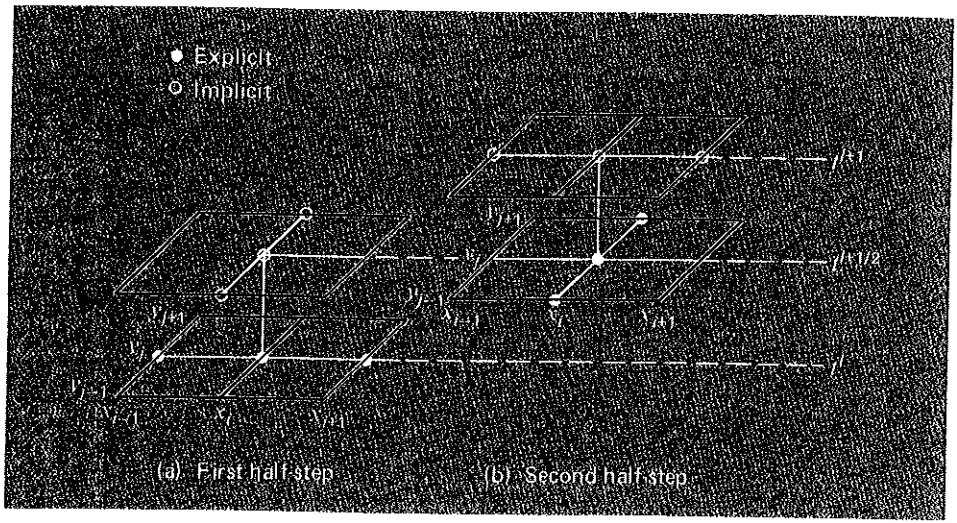

Figure 24.10
The two half-steps used in implementing the alternating-direction implicit scheme for solving parabolic equations in two spatial dimensions.

$$\frac{T_{i,j}^{l+1/2} - T_{i,j}^{l}}{\Delta t/2} = k\left[\frac{T_{i+1,j}^{l} - 2T_{i,j}^{l} + T_{i-1,j}^{l}}{(\Delta x)^2} + \frac{T_{i,j+1}^{l+1/2} - 2T_{i,j}^{l+1/2} + T_{i,j-1}^{l+1/2}}{(\Delta y)^2}\right] \tag{24.19a}$$

Thus, the approximation of $\partial^2 T/\partial x^2$ is written explicitly—that is, at the base point t^l where values of temperature are known. Consequently, only the three temperature terms in the approximation of $\partial^2 T/\partial y^2$ are unknown. For the case of a square grid ($\Delta y = \Delta x$), this equation can be expressed as

$$-\lambda T_{i,j-1}^{l+1/2} + 2(1 + \lambda)T_{i,j}^{l+1/2} - \lambda T_{i,j+1}^{l+1/2} = \lambda T_{i-1,j}^{l} + 2(1 - \lambda)T_{i,j}^{l} + \lambda T_{i+1,j}^{l} \tag{24.19b}$$

which, when written for the system, results in a tridiagonal set of simultaneous equations.

For the second step from $t^{l+1/2}$ to t^{l+1}, Eq. (24.18) is approximated by

$$\frac{T_{i,j}^{l+1} - T_{i,j}^{l+1/2}}{\Delta t/2} = k\left[\frac{T_{i+1,j}^{l+1} - 2T_{i,j}^{l+1} + T_{i-1,j}^{l+1}}{(\Delta x)^2} + \frac{T_{i,j+1}^{l+1/2} - 2T_{i,j}^{l+1/2} + T_{i,j-1}^{l+1/2}}{(\Delta y)^2}\right] \tag{24.20}$$

In contrast to Eq. (24.19a), the approximation of $\partial^2 T/\partial x^2$ is now implicit. Thus, the bias introduced by Eq. (24.19a) will be partially corrected. For a square grid, Eq. (24.20) can be written as

$$-\lambda T_{i-1,j}^{l+1} + 2(1 + \lambda)T_{i,j}^{l+1} - \lambda T_{i+1,j}^{l+1} = \lambda T_{i,j-1}^{l+1/2} + 2(1 - \lambda)T_{i,j}^{l+1/2} + \lambda T_{i,j+1}^{l+1/2} \tag{24.21}$$

Again, when written for a two-dimensional grid, the equation results in a tridiagonal system (Fig. 24.11). As in the following example, this leads to an efficient numerical solution.

EXAMPLE 24.5 A.D.I. method

Problem Statement: Use the A.D.I. method to solve for the temperature of the plate in Examples 23.1 through 23.3. At $t = 0$ assume that the temperature of the plate is zero and the boundary temperatures are instantaneously brought to the levels shown in Fig. 23.4. Employ a time step of 10 s. Recall from Example 24.1, that the coefficient of thermal diffusivity for aluminum is $k = 0.835$ cm^2/s.

Solution: A value of $\Delta x = 10$ cm was employed to characterize the 40 × 40 cm plate from Examples 23.1 through 23.3. Therefore, $\lambda = 0.835(10)/(10)^2 = 0.0835$. For the first step to $t = 5$ (Fig. 24.11*a*), Eq. (24.19*b*) is applied to nodes (1,1), (1,2), and (1,3) to yield the following tridiagonal equations

$$\begin{bmatrix} 2.167 & -0.0835 & 0 \\ -0.0835 & 2.167 & -0.0835 \\ 0 & -0.0835 & 2.167 \end{bmatrix} \begin{Bmatrix} T_{1,1} \\ T_{1,2} \\ T_{1,3} \end{Bmatrix} = \begin{Bmatrix} 6.2625 \\ 6.2625 \\ 14.6125 \end{Bmatrix}$$

which can be solved for

$$T_{1,1} = 3.0160 \qquad T_{1,2} = 3.2708 \qquad T_{1,3} = 6.8692$$

In a similar fashion, tridiagonal equations can be developed and solved for

$$T_{2,1} = 0.1274 \qquad T_{2,2} = 0.2900 \qquad T_{2,3} = 4.1291$$

and

$$T_{3,1} = 2.0181 \qquad T_{3,2} = 2.2477 \qquad T_{3,3} = 6.0256$$

Figure 24.11
The A.D.I. method only results in tridiagonal equations, if it is applied along the dimension that is implicit. Thus, on the first step (*a*), it is applied along the *y* dimension and, on the second step (*b*), along the *x* dimension. These "alternating directions" are the root of the method's name.

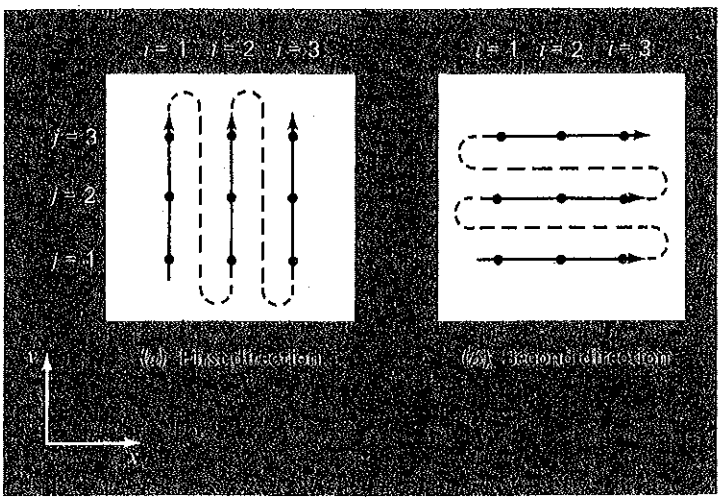

For the second step to $t = 10$ (Fig. 24.11*b*), Eq. (24.21) is applied to nodes (1,1), (2,1), and (3,1) to yield

$$\begin{bmatrix} 2.167 & -0.0835 & 0 \\ -0.0835 & 2.167 & -0.0835 \\ 0 & -0.0835 & 2.167 \end{bmatrix} \begin{Bmatrix} T_{1,1} \\ T_{2,1} \\ T_{3,1} \end{Bmatrix} = \begin{Bmatrix} 12.0639 \\ 0.2577 \\ 8.0619 \end{Bmatrix}$$

which can be solved for

$$T_{1,1} = 5.5855 \qquad T_{2,1} = 0.4782 \qquad T_{3,1} = 3.7388$$

Tridiagonal equations for the other rows can be developed and solved for

$$T_{1,2} = 6.1683 \qquad T_{2,2} = 0.8238 \qquad T_{3,2} = 4.2359$$

and

$$T_{1,3} = 13.1120 \qquad T_{2,3} = 8.3207 \qquad T_{3,3} = 11.3606$$

The computation can be repeated, and the results for $t = 100$, 200, and 300 s are depicted in Fig. 24.12*a* through *c*. As expected, the temperature of the plate rises. After a sufficient time elapses, the temperature will approach the steady-state distribution of Fig. 23.5.

The A.D.I. method is but one of a group of techniques called *splitting methods*. Some of these represent efforts to circumvent shortcomings of A.D.I. For example, it is difficult to directly extend the A.D.I. method to three dimensions by using approximations at $l + 1/3$ and $l + 2/3$. Discussion of other splitting methods as well as more information on A.D.I. can be found elsewhere (Ferziger, 1981; Lapidus and Pinder, 1982).

(*a*) $t = 100$ s (*b*) $t = 200$ s (*c*) $t = 300$ s

Figure 24.12
Solution for the heated plate from Example 24.4 at (*a*) $t = 100$ s, (*b*) $t = 200$ s, and (*c*) $t = 300$ s.

PROBLEMS

Hand Calculations

24.1 Repeat Example 24.1 but for the case where the rod is initially at 100 °C and the derivative at $x = 0$ is equal to 1 and at $x = 10$ is equal to 0.

24.2 Repeat Example 24.1 but for a time step of $\Delta t = 0.05$ s. Compute results to $t = 0.2$ and compare with those in Example 24.1.

24.3 Repeat Example 24.2 but for the case where the derivative at $x = 10$ is equal to zero.

24.4 Repeat Example 24.3 but for $\Delta x = 2.5$ cm.

24.5 Repeat Example 24.5 but for the plate in Fig. P23.3.

24.6 The advection-diffusion equation is used to compute the distribution of concentration along the length of a rectangular chemical reactor (see Case Study 26.1),

$$\frac{\partial c}{\partial t} = D\frac{\partial^2 c}{\partial x^2} - U\frac{\partial c}{\partial x} - kc$$

where c is concentration (mg/m^3), t = time (min), D is a diffusion coefficient (m^2/min), x is distance along the tank's longitudinal axis (m) where $x = 0$ at the tank's inlet, U is velocity in the x direction (m/min), and k is a reaction rate (min^{-1}) whereby the chemical decays to another form. Develop an explicit scheme to solve this equation numerically.

Computer-Related Problems

24.7 Develop a user-friendly computer program for the simple explicit method from Sec. 24.2. Test it by duplicating Example 24.1.

24.8 Modify the program in Prob. 24.7 so that it employs derivative boundary conditions.

24.9 Develop a user-friendly computer program to implement the simple implicit scheme from Sec. 24.3. Test it by duplicating Example 24.2.

24.10 Develop a user-friendly computer program to implement the Crank-Nicolson method from Sec. 24.4. Test it by duplicating Example 24.3.

24.11 Develop a user-friendly computer program for the A.D.I. method described in Sec. 24.5. Test it by duplicating Example 24.5.

Margaret and Gabriel Chapra
Helen and Chester Canale

Formerly published under the title of Numerical Methods for Engineers with Personal Computer Applications, © 1985, by McGraw-Hill, Inc.

NUMERICAL METHODS FOR ENGINEERS

1234567890 HALHAL 89321098

ISBN 0-07-079984-9

This book was set in Times Roman by Publication Services.
The editors were Anne T. Brown and Steven Tenney;
the production supervisor was Friederich W. Schulte;
the designer was Charles Carson.
Cover photograph by Paul Perry.
Drawings were done by J&R Services, Inc.
Arcata Graphics/Halliday was printer and binder.

Library of Congress Cataloging-in-Publication Data

Chapra, Steven C.
Numerical methods for engineers.

Bibliography: p.
Includes index.
1. Engineering mathematics—Data processing.
2. Numerical calculations—Data processing. 3. Microcomputers—Programming. I. Canale, Raymond P.
II. Title.
TA345.C47 1988 511'.02462 88-523
ISBN 0-07-079984-9
ISBN 0-07-010674-6 (solutions manual)
ISBN 0-07-834447-6 (disc)